

Spectral Mismatch Uncertainty Estimation in Solar Cell Calibration Using Monte Carlo Simulation

Kinza Maham , Petri Kärhä , and Erkki Ikonen 

Abstract—A solar cell is characterized using a solar simulator and a reference cell in accordance with standard testing conditions. Deviations between the spectral responsivities of the reference cell and the cell being studied, and deviations of the spectral irradiance of the light source used from the specified air mass 1.5 introduce systematic errors in the calibration of solar cells. These errors are corrected with the so-called spectral mismatch (SMM) correction factor. We demonstrate a Monte Carlo simulation-based analysis of the uncertainties present in an SMM correction factor taking into account the possible spectral correlations of the input parameters, such as the spectral irradiance and the spectral responsivities of the reference cell and the solar cell under test. We also perform a detailed uncertainty analysis of the subcomponents of the SMM factor mainly arising from the spectral irradiance incident on the solar cell. In order to test our estimates, we present a comparison of the uncertainties by six other independent calculations carried out by other institutes. We obtain the worst-case, average, and best-case scenario uncertainties of the SMM correction factor by assuming components to be severely correlated, partially correlated, and not correlated, respectively. The corresponding expanded uncertainties ($k = 2$) are 1.26%, 0.44%, and 0.06%. The worst- and best-case uncertainties lie at the maximum and minimum extremes of the uncertainties estimated by the participants, while the uncertainty estimate obtained assuming partial correlations is close to the median and mean of all results.

Index Terms—Monte Carlo, photovoltaic, solar cell, spectral mismatch (SMM) factor, uncertainty.

I. INTRODUCTION

THE efficiencies of solar cells are characterized using solar simulators and reference cells. The most common solar simulators used to characterize solar cells consist of a steady-state or flashing Xenon arc lamp [1], [2]. In solar cell calibration, measurements are carried out in standard test conditions (STCs). STC specifies an irradiance level of 1000 W/m^2 , cell temperature

Manuscript received 8 February 2023; revised 17 May 2023 and 10 July 2023; accepted 31 August 2023. Date of publication 18 September 2023; date of current version 7 November 2023. This work was supported by the Academy of Finland Flagship Programme, Photonics Research and Innovation (PREIN) under Grant 320167. The projects 16ENG02 (PV-Enerate) and 19ENG01 (Metro-PV) leading to this publication have received funding from the EMPIR Programme cofinanced by the Participating States and the European Union's Horizon 2020 Research and Innovation Programme. (Corresponding author: Kinza Maham.)

Kinza Maham and Petri Kärhä are with Metrology Research Institute, Aalto University, 00076 Aalto, Finland (e-mail: kinza.maham@aalto.fi; petri.karha@aalto.fi).

Erkki Ikonen is with Metrology Research Institute, Aalto University, 00076 Aalto, Finland, and also with VTT MIKES Metrologia, 02044 Espoo, Finland (e-mail: erkki.ikonen@aalto.fi).

Color versions of one or more figures in this article are available at <https://doi.org/10.1109/JPHOTOV.2023.3311890>.

Digital Object Identifier 10.1109/JPHOTOV.2023.3311890

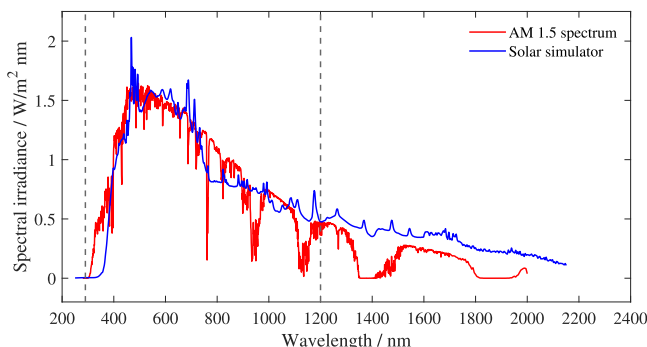


Fig. 1. Spectral irradiance of the xenon–halogen solar simulator and the standardized AM1.5 spectrum. The approximate range of the measured responsivity of solar cells is indicated by the dashed lines.

of 25°C , and a reference spectrum as defined in IEC 60904-3 air mass 1.5 global (AM1.5) [3].

In the calibration of the output under STC, the response of the unknown solar cell is compared to that of the reference solar cell with known spectral responsivity. This gives the solar cell responsivity in A/W provided that the simulator spectrum used to produce STC is identical to the reference spectrum AM1.5 or the reference and the device under test (DUT) have identical spectral responsivities. Deviations between the spectral responsivities of the reference cell and the cell being studied, and deviations of the spectral irradiance of the light source used from the specified AM1.5 introduce a systematic deviation in the calibration of the solar cell (Fig. 1). This error is corrected with the so-called spectral mismatch (SMM) factor [4], [5].

The input parameters of SMM factor calculation have uncertainties that can be combined to evaluate the uncertainty due to SMM. The SMM uncertainty has been analyzed by Reichmuth et al. [6] and Mühleis [7] previously. The input parameters are spectral responsivities of the reference cell and the cell under test and the spectral irradiance of the solar simulator. The uncertainties of spectral responsivities are determined by calibration measurements, while the uncertainty components of spectral irradiance can be further subdivided into components, such as radiometric calibration, stability, bandwidth, wavelength, and noise.

This article presents a method to analyze uncertainty due to SMM using Monte Carlo analysis. The input parameters are wavelength dependent and may contain unknown correlations among wavelengths. The analysis considers possible correlations and gives estimates for the worst-case, best-case, and the

average uncertainties due to the SMM. The way of considering correlations in the input parameters is based on the method proposed earlier by Kärh a et al. [8], [9] and applied also to atmospheric ozone retrieval [10]. It should be noted that the approach is more general than the covariance methods based on the (linear) Pearson correlation coefficient. The rest of this article is organized as follows. The methodology is presented in Section II, followed by introducing the input parameters in Section III. The results of the uncertainty simulations are given in Section IV. Six other institutes have performed uncertainty analysis using the same input parameters but widely differing methods. In Section V, we compare our results with the other participating institutes. Finally, Section VI concludes this article.

II. UNCERTAINTY MODEL

The factor describing SMM is calculated as [4], [5], [11] follows:

$$\text{SMM} = \frac{\int_{\lambda} E_{\text{Ref}}(\lambda) \cdot S_{\text{Ref}}(\lambda) d\lambda}{\int_{\lambda} E(\lambda) \cdot S_{\text{Ref}}(\lambda) d\lambda} \cdot \frac{\int_{\lambda} E(\lambda) \cdot S_{\text{DUT}}(\lambda) d\lambda}{\int_{\lambda} E_{\text{Ref}}(\lambda) \cdot S_{\text{DUT}}(\lambda) d\lambda} \quad (1)$$

where λ is the wavelength (290–1200 nm) over which SMM is calculated, $E_{\text{Ref}}(\lambda)$ is the reference solar spectrum AM1.5, $E(\lambda)$ is the spectrum of the solar simulator, $S_{\text{Ref}}(\lambda)$ is the spectral responsivity of the reference cell, and $S_{\text{DUT}}(\lambda)$ is the spectral responsivity of the unknown test cell. Parameters $E(\lambda)$, $S_{\text{Ref}}(\lambda)$, and $S_{\text{DUT}}(\lambda)$ have been measured, and they have known spectrally varying uncertainties, as described in more detail in Section III. Correlations between the parameter values at different wavelengths are unknown.

Both the reference cell and the cell under test are based on silicon. They give very little signal in the UV region for solar radiation; thus, the lower wavelength limit of 290 nm was considered short enough for calculations. The DUT has its peak responsivity already at 600 nm; thus, 1200 nm was considered long enough as the upper wavelength limit. Possible missing data were extrapolated, and additional data were ignored in the calculations. All data were also interpolated to a 1-nm interval.

Possible correlations are taken into account by forming a wavelength-dependent error function used to distort the spectrally varying input parameters. In the case of $S_{\text{Ref}}(\lambda)$, the equation takes the form [8]

$$S_{\text{Ref},e}(\lambda) = [1 + \delta(\lambda) \cdot u(\lambda)] \cdot S_{\text{Ref}}(\lambda) \quad (2)$$

where $S_{\text{Ref},e}(\lambda)$ is the distorted spectral responsivity and $u(\lambda)$ is the relative standard uncertainty of $S_{\text{Ref}}(\lambda)$. The deviation $\delta(\lambda) \cdot u(\lambda)$ will go through all the spectral shapes that the uncertainty allows, where $\delta(\lambda)$ is the error function that is used to add deviation to $S_{\text{Ref}}(\lambda)$ in the Monte Carlo simulation to form the distorted spectral responsivity. The uncertainty of $S_{\text{DUT}}(\lambda)$ and of the subcomponents of $E(\lambda)$ are analyzed in the same way.

The error function $\delta(\lambda)$ is constructed analogically to Fourier analysis by summing orthogonal basis functions $f_i(\lambda)$ as

$$\delta(\lambda) = \sum_{i=0}^N \delta_i f_i(\lambda) \quad (3)$$

where $N + 1$ is the number of basis functions included and δ_i are the weights. The variances of the basis functions are set to unity by requiring that $\int f_i^2(\lambda) d\lambda / (\lambda_2 - \lambda_1) = 1$. To account for the full correlation, function $f_0(\lambda) = 1$ is used. For weights δ_i , we also require that $\sum_{i=0}^N \delta_i^2 = 1$. The basis functions are selected as

$$f_i(\lambda) = \sqrt{2} \sin \left[i \left(2\pi \frac{\lambda - \lambda_1}{\lambda_2 - \lambda_1} \right) + \phi_i \right] \quad (4)$$

where index $i = 1, 2, 3, \dots, N$, wavelengths λ_1 and λ_2 are 290 nm and 1200 nm, respectively, and ϕ_i is the phase of the basis function. The phase is equally distributed between 0 and 2π . Basis functions selected this way are orthogonal and fulfill the requirement of variance being unity.

The weights are generated in an $(N+1)$ -dimensional spherical coordinate system [12]. First, $N+1$ Gaussian random variables $Y_0, Y_1, \dots, Y_N \sim N(0,1)$ are selected. Weights are then calculated as

$$\delta_i = \frac{Y_i}{\sqrt{Y_0^2 + Y_1^2 + \dots + Y_N^2}}. \quad (5)$$

Parameter N is varied between 0 and the Nyquist criterion value [13], [14]. The maximum of N is equal to half of the number of data points. Data from 290 to 1200 nm at 1-nm interval contain 911 data points; thus, $N = 456$. At each N , thousands of scenarios with varied Y_i and ϕ_i are calculated, and the standard deviation of the resulting SMM factors is calculated. This standard deviation represents the uncertainty caused by the spectral input quantities under analysis assuming varied correlation scenarios.

III. CONTRIBUTING INPUT PARAMETERS

Fig. 1 presents the standardized spectral irradiance AM1.5 and the spectral irradiance of the solar simulator. The solar simulator used is the Wacom steady-state xenon–halogen solar simulator of the Joint Research Center–European Solar Test Installation, Italy [15].

The spectral irradiance of the AM1.5 has by definition no measurement uncertainty. Uncertainty of the spectral irradiance of the solar simulator and the uncertainties of the individual components contributing to it are plotted in Fig. 2. As can be seen, uncertainties in wavelength and bandwidth are the highest contributing components.

The uncertainties related to the radiometric calibration, stability, bandwidth, wavelength, and signal-to-noise ratio (SNR) originate from the calibration of the spectroradiometer used to measure the spectral irradiance of the solar simulator. The detailed calibration method and the calculation of the uncertainties can be found in [15] and [16]. Three spectroradiometers were used in the measurements at three wavelength ranges, 250–1000 nm, 1000–1600 nm, and 1600–2150 nm. The resulting wavelength uncertainties are 0.2 nm, 0.8 nm, and 1 nm, respectively.

The spectral irradiance data were corrected for bandwidth. The bandwidth uncertainty was estimated in [16] using Monte Carlo simulation by varying the measured deviations around the triangular bandpass function. The method used for bandwidth correction may introduce a systematic bias. An alternative approach that can be used to deconvolute the measured spectra

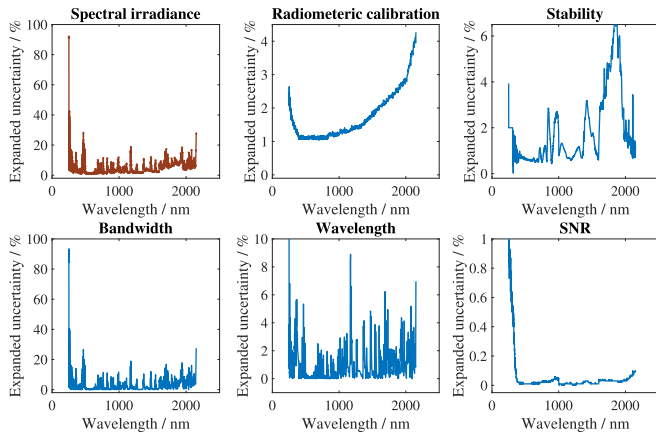


Fig. 2. Relative expanded uncertainties ($k = 2$) in the spectral irradiance of the solar simulator and its subcomponents: radiometric calibration, stability, bandwidth, wavelength, and SNR [15], [16]. Spectral irradiance uncertainty is the square root of the sum of squares of the subcomponent uncertainties. Note the significantly different vertical scales for the different curves.

is proposed by Eichstädt et al. [17]. However, for the present analysis, we use the uncertainties calculated in [16].

The uncertainties in wavelength have been converted to their effects on the spectral irradiance values measured for the solar simulator at the corresponding wavelengths. In our analysis, these uncertainties in spectral irradiance were used as $u(\lambda)$ in (2) when analyzing spectral irradiance.

A significant uncertainty component of a solar simulator may be the spatial uniformity of the spectral irradiance that produces a correction factor to the irradiance $E(\lambda)$ of (1), depending on the sizes and spatial responsivity uniformities of the reference cell and DUT. As a first-order approximation, which is used in this work, the correction factor is the same at all wavelengths and disappears from (1). We have excluded from the analysis also the other geometrical and electrical effects, which influence in the same way at all wavelengths.

The used reference solar cell is made of n-type crystalline silicon (c-Si) encapsulated and the DUT is made of amorphous silicon (a-Si). The spectral responsivities of the reference cell and the DUT have been measured over the wavelength ranges of 280–1200 nm and 290–1000 nm, respectively. These spectral responsivities are presented in Fig. 3. The spectral responsivity of the reference cell is significantly larger than the spectral responsivity of DUT at a part of the common spectral range. In real measurement, this would not be preferable, but the cells have been chosen to increase the SMM intentionally and, thus, to enhance possible differences in its calculation.

The estimated uncertainties of the spectral responsivities are shown in Fig. 4. The relative expanded uncertainty of the DUT in the range of 1000–1200 nm is conservatively estimated to be 100% (not shown in Fig. 4).

IV. SIMULATION RESULTS

The SMM factor was determined to have a value of 0.9964. The deviation from unity is due to the mismatch between the

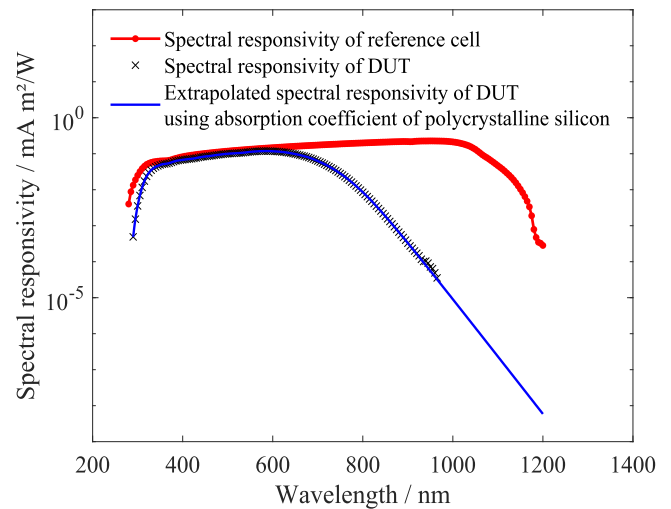
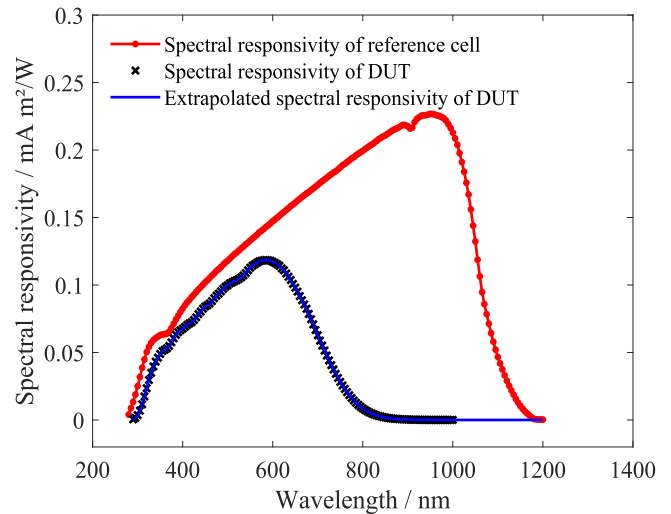


Fig. 3. Spectral responsivity of the reference cell and the DUT, in linear and logarithmic scales. DUT's spectral responsivity was extrapolated to match the wavelength range of the reference cell's spectral responsivity, using a model based on the absorption coefficient of polycrystalline silicon [18].

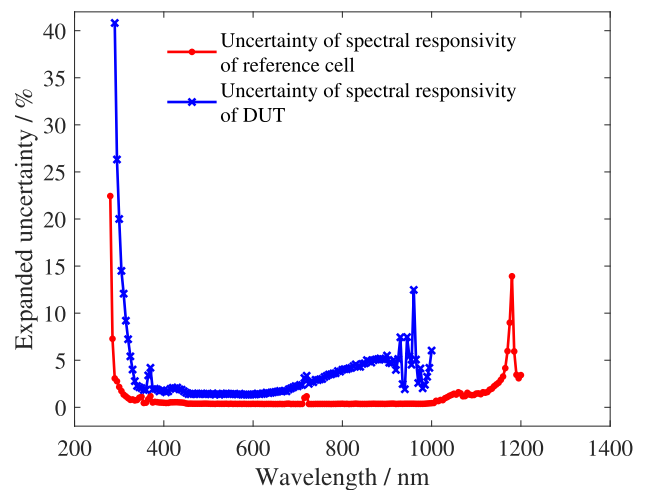


Fig. 4. Relative expanded uncertainties ($k = 2$) of the spectral responsivities of the reference cell and the DUT.

TABLE I
STANDARD UNCERTAINTIES (IN %) OF THE SMM CORRECTION FACTOR CAUSED BY THE SUBCOMPONENTS OF THE SPECTRAL IRRADIANCE OF THE SOLAR SIMULATOR: RADIOMETRIC CALIBRATION, STABILITY, BANDWIDTH, WAVELENGTH, AND SNR OF THE SPECTRORADIOMETER USED TO MEASURE THE LIGHT SOURCE; AND RESPONSIVITIES OF THE REFERENCE CELL AND THE DUT

N	Radiometric calibration	Stability	Bandwidth	Wavelength	SNR	Responsivity of reference cell	Responsivity of DUT	Quadratic sum
0	0.0000	0.0000	0.0000	0.0000	0.0000	0.0000	0.0000	0.0000
1	0.0170	0.1767	0.0377	0.0045	0.0032	0.0007	0.0317	0.1843
2	0.2756	0.2876	0.4676	0.1181	0.0053	0.0025	0.0359	0.6266
3	0.1563	0.1856	0.4276	0.1182	0.0033	0.0100	0.0544	0.5087
4	0.1132	0.1362	0.2964	0.0877	0.0023	0.0059	0.0485	0.3596
5	0.1008	0.1135	0.1316	0.0520	0.0021	0.0135	0.0533	0.2147
6	0.0851	0.1114	0.1016	0.0432	0.0022	0.0152	0.0554	0.1875
7	0.0822	0.1152	0.2078	0.0629	0.0019	0.0137	0.0526	0.2648
8	0.0768	0.0899	0.2258	0.0614	0.0017	0.0099	0.0493	0.2670
9	0.0710	0.0855	0.1672	0.0440	0.0016	0.0114	0.0497	0.2118
10	0.0665	0.0922	0.0863	0.0253	0.0015	0.0094	0.0438	0.1517
16	0.0544	0.0687	0.0946	0.0336	0.0012	0.0063	0.0305	0.1369
32	0.0382	0.0481	0.0659	0.0211	0.0008	0.0036	0.0170	0.0942
50	0.0308	0.0382	0.0634	0.0190	0.0007	0.0031	0.0127	0.0834
64	0.0274	0.0344	0.0559	0.0175	0.0006	0.0029	0.0130	0.0745
75	0.0254	0.0319	0.0486	0.0152	0.0006	0.0025	0.0110	0.0662
100	0.0218	0.0274	0.0428	0.0135	0.0006	0.0025	0.0100	0.0578
128	0.0194	0.0241	0.0378	0.0110	0.0004	0.0020	0.0089	0.0509
150	0.0178	0.0226	0.0337	0.0109	0.0004	0.0018	0.0082	0.0464
175	0.0166	0.0207	0.0326	0.0104	0.0004	0.0017	0.0076	0.0440
200	0.0155	0.0194	0.0299	0.0096	0.0003	0.0016	0.0070	0.0407
256	0.0137	0.0169	0.0257	0.0085	0.0003	0.0016	0.0063	0.0353
280	0.0131	0.0163	0.0268	0.0079	0.0003	0.0014	0.0061	0.0355
300	0.0126	0.0158	0.0272	0.0073	0.0003	0.0013	0.0055	0.0351
375	0.0113	0.0142	0.0225	0.0068	0.0002	0.0012	0.0051	0.0302
456	0.0104	0.0127	0.0191	0.0064	0.0002	0.0010	0.0046	0.0264

First column indicates the number of the highest order basis function included in the analysis. Quadratic sum refers to the square root of the sum of squares of the terms in the seven middle columns.

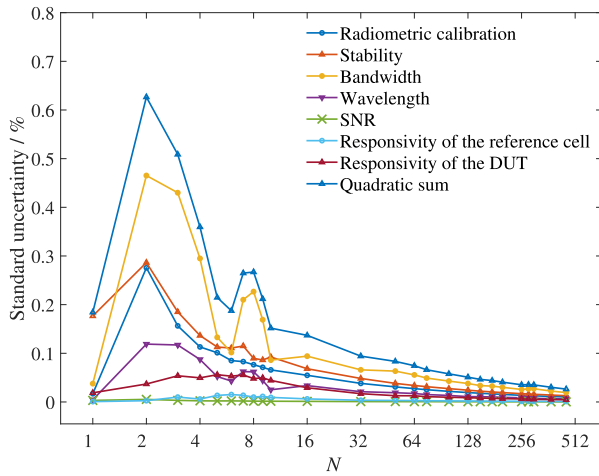


Fig. 5. Uncertainties caused in SMM factor by the contributing components.

spectral responsivities of the reference cell and the DUT, and the deviation of the solar simulator spectrum from AM1.5.

The uncertainty was simulated at a 1-nm interval in the wavelength range of 290–1200 nm using the methods of Section II. According to the Nyquist theorem, the maximum number of basis functions N was limited to 456, half of the number of spectral measurement points. The uncertainty analysis was carried out separately for all subcomponents contributing to the uncertainty of the SMM factor. Table I presents the results for the

subcomponents of spectral irradiance; radiometric calibration, stability, bandwidth, wavelength, and SNR; and the responsivity of the reference cell and the DUT.

As can be seen, the uncertainties are zero with the first component $f_0(\lambda)$ describing fully correlated uncertainties. Full correlation leads to a constant factor in front of $S_{\text{Ref}}(\lambda)$, $S_{\text{DUT}}(\lambda)$, or $E(\lambda)$ in (1). Thus, a full correlation would lead to an uncertainty of zero and is included in the analysis as a mathematical case that can be used as a contribution to the uncertainty evaluation. Full correlation may be due to wrong distance or wrong aperture area during the spectral responsivity calibration that affects the results at all wavelengths in the same way.

The standard uncertainties of the subcomponents of spectral irradiance, responsivity of reference cell, and responsivity of DUT are plotted in Fig. 5 as a function of N and given in the numerical form in Table I. The highest uncertainties are observed at $N = 2$.

It is surprising how little the responsivities of the cells contribute to the uncertainty, as compared with the components of the spectral irradiance. We conclude that this is due to the poor match of the reference cell to the DUT, as seen in Fig. 3. In addition to increasing the value of SMM, it also seems to increase the uncertainties caused by the measurement of spectral irradiance. The matching of the solar simulator to the reference spectrum is much better, as seen in Fig. 1. Then, the uncertainties in spectral responsivities are not amplified in the same way as spectral irradiance uncertainties with poor match of cell responsivities.

TABLE II

UNCERTAINTY BUDGETS OF SMM CORRECTION FACTOR ASSUMING THREE DIFFERENT SCENARIOS FOR CORRELATIONS: SEVERE ($N = 2$ FOR IRRADIANCE COMPONENTS AND $N = 6$ FOR RESPONSIVITIES), NO CORRELATION ($N = 456$ FOR IRRADIANCE COMPONENTS AND $N = 100$ FOR RESPONSIVITIES), AND PARTIAL CORRELATION (AVERAGE OF $N = 0, 2$, OR 6 , AND 456 OR 100) OBTAINED AS A COMBINATION OF THE OTHER CASES

Source of uncertainty	Correlation		
	Severe	None	Partial
Radiometric calibration	0.276	0.010	0.095
Stability	0.288	0.013	0.100
Bandwidth	0.468	0.019	0.162
Wavelength	0.118	0.006	0.042
Spectral responsivity of reference cell	0.015	0.003	0.006
Spectral responsivity of DUT	0.055	0.010	0.022
Combined standard uncertainty	0.63	0.03	0.22
Expanded uncertainty ($k = 2$)	1.26	0.06	0.44

Values for uncertainty components (in %) have been taken from Table I.

Table II presents the expanded uncertainty in the SMM factor due to the largest subcomponents of spectral irradiance, the responsivity of the reference cell, and the responsivity of the DUT. We have estimated three different scenarios for correlations. In the first case, we assumed that all parameters are severely correlated (i.e., it leads to maximum uncertainty). For this, we have chosen the highest standard uncertainties obtained from the Monte Carlo analysis in Table I. This gives us an expanded uncertainty of 1.26%. In the case of no correlation, we have considered the standard uncertainties at $N = 456$ and at $N = 100$ for responsivities (due to interpolation from 5-nm spectral interval to 1-nm interval), resulting in an expanded uncertainty of 0.06%. At high N values, the generated error functions resemble noise, as was shown in [8] and [10].

The third case, partial correlation, considers likely uncertainties calculated as the average of the fully correlated, severely correlated, and uncorrelated uncertainties, which results in an expanded uncertainty of 0.44%. For this, we take the average of uncertainties at $N = 0$, $N = 2$ (or at $N = 6$ for responsivity), and $N = 456$ (or at $N = 100$ for responsivity), respectively. Inclusion of the case $N = 0$ in the average is crucial, and we describe in the following text why such an average should be taken.

The third case assumption is based on the degrees of equivalence in CCPR-K1, a key comparison studied in [9]. On average, the deviations of National Standards' Laboratories from the key comparison reference values show three types of behavior: First, errors independent of wavelength, originating, e.g., from geometrical settings; second, random errors originating from noise; and third, spectrally complicated structures originating, e.g., from interpolations and extrapolations carried out in scale realizations. The chosen approach of averaging effects of uncertainties based on assuming fully correlated, severely correlated, and noncorrelated spectral behavior with equal weights corresponds to this noted behavior. Noncorrelated errors (noise) are actually very small in the measurements of National Standard Laboratories but get enhanced in further measurements. This is well demonstrated by the components, as listed in Fig. 2.

TABLE III

COMPARISON OF OUR OBTAINED UNCERTAINTIES WITH OTHER CALCULATIONS

Participant	SMM	U(SMM)/%
Aalto (severe correlation)	0.99640	1.26%
#2	0.99635	0.80%
#6	0.99634	0.51%
#1	0.99630	0.47%
Aalto (partial correlation)	0.99640	0.44%
#3	0.99640	0.30%
#4	0.99636	0.14%
#5	0.99640	0.14%
Aalto (no correlation)	0.99640	0.06%

All uncertainties are given as expanded uncertainties ($k = 2$ indicating 95% confidence level).

V. COMPARISON WITH OTHER CALCULATIONS

This work was carried out as a part of EU-funded projects, PV-Enerate and Metro-PV. Six other institutes also estimated the SMM factor and its uncertainty, according to the Guide to the Expression of Uncertainty in Measurement [19]. Correlations between the input quantities were not given, so each institute had to make its own assumptions. Table III presents the comparison of our results with the results obtained by the other six participants. Good agreement between the SMM values of participants indicates that the chosen wavelength region for integration is wide enough for each participant.

Correlations were taken into account by each participant; however, the assumptions varied. The deviations of the results indicate that people interpret correlations differently. With our method, we obtained and listed three uncertainties. Our worst-case (severe correlations) and best-case (no correlations) estimates with values of 1.26% and 0.06% locate at the extremes of the comparison. The average uncertainty value of 0.44% locates at the median and close to the mean of results #1-#6.

VI. CONCLUSION

We presented a method to estimate the uncertainties of the SMM correction factor using Monte Carlo simulation. The method takes into account possible correlations of wavelength-dependent quantities. As input data, uncertainties in the spectral irradiance of the light source, spectral responsivities of the reference cell, and the cell under test were considered. Separate uncertainty components of spectral irradiance are also considered in this analysis. The most significant sources of uncertainty arise from measuring the irradiance of the simulator. Large contributions include uncertainties related to the bandwidth correction and stability of the spectrometer used for measuring spectra, as well as uncertainties related to the calibration of the spectrometer itself. Three correlation scenarios, worst case, best case, and average, were considered. The corresponding expanded uncertainties of SMM correction factor were 1.26%, 0.06%, and 0.44%, respectively.

The uncertainties obtained were compared with independent calculations of six other institutes. Due to the requirements of the round robin and full comparability of the results of all

participants, a wavelength range of 290–1200 nm was chosen for the calculation of the value of SMM correction factor and the corresponding uncertainty. Our worst-case and best-case uncertainties lie in the extremes of the comparison, marking maximum and minimum uncertainties of SMM correction factor. Our average scenario uncertainty is close to the mean and median of all results.

VI. ACKNOWLEDGMENT

The authors would like to thank I. Kröger and S. Winter of the Physikalisch-Technische Bundesanstalt for providing data and commenting the work, M. Mühleis (FhG), G. Jüngst, and A. Vegas (INTA), D. Hinken (ISFH), H. Müllejans (JRC), and G. Bellenda (SUPSI) for providing uncertainty estimates, and A. Vaskuri for her contribution to the Monte Carlo software.

VI. DATA AVAILABILITY

The data and software that support the findings of this study are openly available at the following URL: <https://doi.org/10.5281/zenodo.4643969>.

REFERENCES

- [1] J. Petrasch et al., “A novel 50 kW 11,000 suns high-flux solar simulator based on an array of xenon arc lamps,” *J. Sol. Energy Eng.*, vol. 129, pp. 405–411, 2007.
- [2] V. Esen, Ş. Sağlam, and B. Oral, “Light sources of solar simulators for photovoltaic devices: A review,” *Renewable Sustain. Energy Rev.*, vol. 77, pp. 1240–1250, 2017.
- [3] *Photovoltaic Devices—Part 3: Measurement Principles for Terrestrial Photovoltaic (PV) Solar Devices With Reference Spectral Irradiance Data*, Int. Electrotech. Commission, Geneva, Switzerland, IEC Standard 60904-3:2019, 2019.
- [4] C. H. Seaman, “Calibration of solar cells by the reference cell method—The spectral mismatch problem,” *Sol. Energy*, vol. 29, no. 4, pp. 291–298, 1982.
- [5] *Photovoltaics Devices—Part 7: Computation of the Spectral Mismatch Correction for Measurements of Photovoltaic Devices*, IEC Standard 60904-7:2019, 2019.
- [6] S. K. Reichmuth et al., “Measurement uncertainties in I–V calibration of multi-junction solar cells for different solar simulators and reference devices,” *IEEE J. Photovolt.*, vol. 10, no. 4, pp. 1076–1083, Jul. 2020.
- [7] M. Mühleis, “Spectral shaping for accurate solar cell characterization,” Doctoral dissertation, Fraunhofer Institute for Solar Energy Systems ISE, Universität Freiburg, Freiburg im Breisgau, Germany, 2022.
- [8] P. Kärhä, A. Vaskuri, H. Mäntynen, and E. Ikonen, “Method for estimating effects of unknown correlations in spectral irradiance data on uncertainties of spectrally integrated colorimetric quantities,” *Metrologia*, vol. 54, pp. 524–534, 2017.
- [9] P. Kärhä, A. Vaskuri, T. Pulli, and E. Ikonen, “Key comparison CCPR-K1.a as an interlaboratory comparison of correlated color temperature,” *J. Phys. Conf. Ser.*, vol. 972, 2018, Art. no. 012012.
- [10] A. Vaskuri, P. Kärhä, L. Egli, J. Gröbner, and E. Ikonen, “Uncertainty analysis of total ozone derived from direct solar irradiance spectra in the presence of unknown spectral deviations,” *Atmos. Meas. Techn.*, vol. 11, pp. 3595–3610, 2018.
- [11] K. Bothe, D. Hinken, B. Min, and B. Schinke, “Accuracy of simplifications for spectral responsivity measurements of solar cells,” *IEEE J. Photovolt.*, vol. 8, no. 2, pp. 611–620, Mar. 2018.
- [12] J. S. Hicks and R. F. Wheeling, “An efficient method for generating uniformly distributed points on the surface of an n-dimensional sphere,” *Commun. ACM*, vol. 2, pp. 17–19, 1959.
- [13] W. Gautschi, *Numerical Analysis*, vol. 2. Boston, MA, USA: Birkhäuser Basel, 1999.
- [14] F. Durand, “A frequency analysis of Monte-Carlo and other numerical integration schemes,” Massachusetts Inst. Technol., Cambridge, MA, USA., 2011.
- [15] R. Galleano, I. Kröger, F. Plag, S. Winter, and H. Müllejans, “Traceable spectral irradiance measurements in photovoltaics: Results of the PTB and JRC spectroradiometer comparison using different light sources,” *Measurement*, vol. 124, pp. 549–559, 2018.
- [16] C. Schinke et al., “Calibrating spectrometers for measurements of the spectral irradiance caused by solar radiation,” *Metrologia*, vol. 57, 2020, Art. no. 065027.
- [17] S. Eichstädt et al., “Comparison of the Richardson–Lucy method and a classical approach for spectrometer bandpass correction,” *Metrologia*, vol. 50, pp. 107–118, 2013.
- [18] A. Danilenko et al., “Characterization of PillarHall test chip structures using a reflectometry technique,” *Meas. Sci. Technol.*, vol. 34, 2023, Art. no. 094006.
- [19] Joint Committee for Guides in Metrology, *Guide to Expression of Uncertainty in Measurement*, BIPM, Paris, France, 2008.